elektron

Revista Elektron, Vol. 10, No. 1, pp. 12–24 (2026)
https://doi.org/10.37537/rev.elektron.10.1.237.2026

Review Article

MOS devices for dosimetry applications

Dispositivos MOS para aplicaciones de dosimetría

L. Sambuco Salomone [#1], S. Carbonetto [#], M. V. Cassani [#], M. A. Garcia-Inza [#†], E. Redin [#], A. Faigón [#]

[#] *Laboratorio de Física de Dispositivos - Microelectrónica, INTECIN, Facultad de Ingeniería, Universidad de Buenos Aires - CONICET*
Av. Paseo Colón 850, CABA, Argentina

[†] *Laboratorio de Nanoelectrónica, Unidad de Investigación y Desarrollo de las Ingenierías (UIDI), Universidad Tecnológica Nacional (UTN-FRBA)*
Medrano 951, CABA, Argentina

[1] lsambuco@fi.uba.ar

Received: 2026-05-06 ; Accepted: 2026-06-10

Abstract—**This work presents a review of metal-oxide-semiconductor (MOS) dosimetry from its physical principles up to the most recent developments. The limitations of MOS dosimeters are analyzed and the usually considered solutions are described. MOS dosimeters based on alternative structures, such as floating gate devices, are also discussed.**

Keywords: Radiation effects; MOSFET; Dosimetry.

Resumen—**Este trabajo presenta una revisión de la dosimetría MOS, desde sus principios físicos hasta los desarrollos recientes. Las limitaciones de los dosímetros MOS son analizadas y las soluciones comúnmente empleadas son descriptas. Dosímetros MOS basados en estructuras alternativas, tales como dispositivos de compuerta flotante, son también discutidos.**

Palabras clave: Efectos de radiación; MOSFET; Dosimetría.

I. Introduction

The growing interest in developing increasingly smaller satellites at ever-decreasing costs [1] has led to continuous changes in the methods for selecting the electronic components to be used, due to their sensitivity to ionizing radiation present in space [2]. This radiation is mostly due to protons (10 MeV – 100 MeV) [3]-[4] and electrons (100 keV – 10 MeV) [5] trapped in the interior and outer Van Allen belts, respectively, but also high-energy galactic cosmic-rays, such as electrons (1 GeV – 1 TeV) which dominate for higher altitudes orbits [6]. Similarly, estimating the radiation received by patients in medical applications such as radiotherapy or diagnostic radiology has resulted in increasingly stringent requirements regarding administered dose levels, demanding uncertainties of less than 3% for each irradiation session [7] and less than 5% for the entire treatment [8]. Radiation sources used in medical applications include X-ray from LINAC (4–25 MeV) [9], γ-rays from ^{60}Co (1.17 and 1.33 MeV) [10] or ^{192}Ir (0.3–0.6 MeV) [11], and protons (70–250 MeV) [12].

MOS dosimetry is based on the use of a MOSFET transistor as an ionizing radiation sensor for dose estimation in harsh environments by means of the progressive shift in the threshold voltage (V_t) as a consequence of the absorbed dose. Compared to other alternatives, the MOS dosimeter offers several advantages, including its small size, which translates into high spatial resolution if a sensor array is employed, its easy integration with readout electronics and/or additional systems, its long data retention time, which allows readings to be taken both during and after irradiation, and the possibility of performing real-time measurements.

This work presents an overview of MOS dosimetry, including its physical principles, main characteristics, limitations and recent developments. This work is organized as follows. Section II describes the physics related to radiation effects on MOS devices. Section III presents the MOS dosimeter based on a single MOSFET transistor, while section IV analyzes the dosimeter based on a floating-gate (FG) structure. Finally, section VI presents the conclusions.

II. Radiation Effects in MOS Devices

When a MOS device is exposed to ionizing radiation, different microscopic processes lead to positive charge accumulation within the oxide and the generation of traps at the substrate/oxide interface, as schematically shown in the band diagram of a MOS structure with a positive bias applied to the gate electrode in Fig. 1. This section describes each one of these processes.

elektron
Revista Elektron, Vol. 10, No. 1, pp. 12–24 (2026)
https://doi.org/10.37537/rev.elektron.10.1.237.2026

Review Article

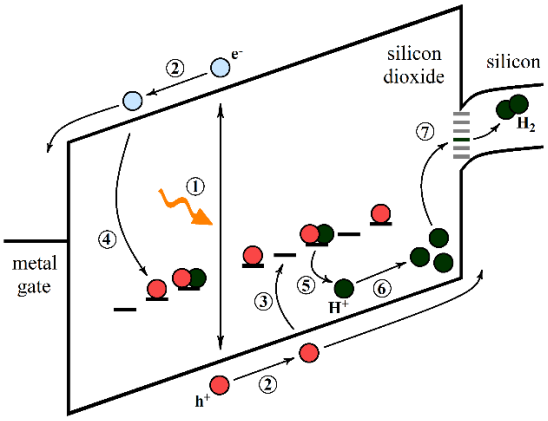

Fig. 1. Band diagram schematic representation of the irradiation of a MOS structure with positive gate bias. ① charge generation and initial recombination, ② electron (blue) and hole (red) transport, ③ hole trapping, ④ trapped hole neutralization through electron trapping, ⑤ proton release from a positively-charged hidrogenated defect, ⑥ proton transport, and ⑦ depassivation of interface trap and release of a hydrogen molecule.

A. Generation and initial recombination

When a material is exposed to ionizing radiation, the incident particle, whether a photon, a high-energy electron, or a proton, deposits energy in different regions of the structure, causing the ionization of atoms and the generation of electron-hole pairs through various mechanisms, such as photoelectric effect, Compton effect, pair production, and Coulomb scattering. The occurrence of these mechanisms depends on the type of particle, its energy, and the atomic number of the target material. In the case of a MOS structure, the response is dominated by what occurs within the oxide layers, and in particular, the gate oxide. In the typical case where the gate oxide is made of SiO_2, the energy required to produce an electron-hole pair is 17 eV, so the resulting density of electron-hole pairs generated per unit dose is $g_0 = 8.1\times10^{12}$ cm^{-3} rad^{-1} [13]-[14].

After their generation, electrons and holes can recombine with each other, depending on numerous factors, such as the type of incident radiation, its energy, and the electric field. In the case of low-energy particles or heavy electrically charged particles, such as protons, the incident particle leaves behind a densely populated column of generated pairs, enabling recombination between electrons and holes from different pairs, which can be represented by the columnar model [13], [15]-[16]. In contrast, for high-energy particles or light particles, such as electrons, the distance between pairs is much greater than the initial distance between electrons and holes in the same pair, meaning that recombination only occurs within the same pair, as represented by the geminate model [17]-[18]. Figure 2 shows the fraction of pairs that escape initial recombination, known as *fractional yield*, as a function of electric field for different radiation sources [19]. Although the mentioned models are reliable, it is common to use semi-empirical analytical expressions, which allows for a simpler analysis of the initial recombination [20].

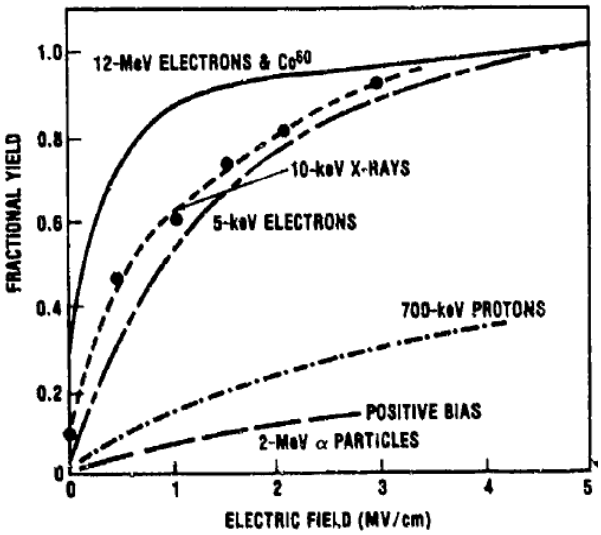

Fig. 2. The fraction of holes that escape initial recombination (*fractional yield*) as a function of electric field for different radiation sources [19].

B. Charge transport

After escaping the initial recombination, the electrons are drifted by the electric field, leaving the oxide in times on the order of picoseconds [21], due to their high mobility [22]-[23].

In contrast, holes exhibit slow, dispersive transport that can span several decades, as shown in Fig. 3. This figure shows the flat-band voltage (V_{FB}) recovery curves at different temperatures after a radiation pulse. The effect of temperature modifies the timescale of the transport process, causing the original curves to overlap when shifted in time, a phenomenon known as universality. This type of transport can be mathematically represented by a continuous-time random walk (CTRW), and its physical origin may be associated with the multiple capture in and release from traps within the oxide [24]-[25], or with a kind of hopping between traps, associated with tunnel transitions between them [26]-[27].

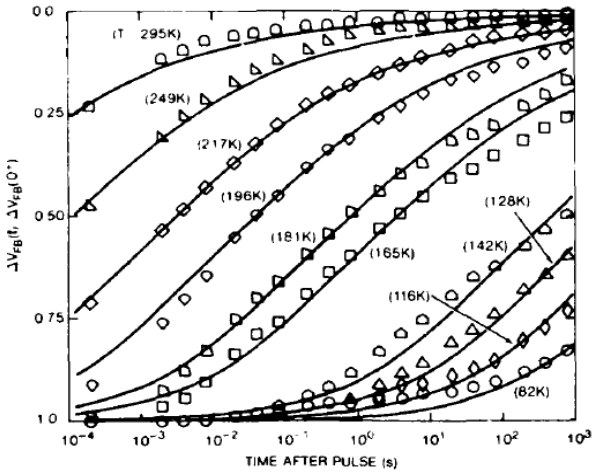

Fig. 3. Flatband voltage recovery after pulsed electron irradiation as a function of time for different temperatures [27].

elektron
Revista Elektron, Vol. 10, No. 1, pp. 12–24 (2026)
https://doi.org/10.37537/rev.elektron.10.1.237.2026
Review Article

C. *Hole capture*

During their transport through the oxide, holes can be captured by defects in a relatively stable manner, meaning that the probability of a hole escaping the trap is sufficiently low for the timescales typically considered in experiments. This characteristic distinguishes this capture process from that associated with dispersive transport, suggesting that these traps are sufficiently separated, allowing for a low probability of transition between them, and are located at deep energy levels so the probability of emission into the valence band is negligible. Hole traps are associated with oxygen vacancies, which exhibit a dimer structure in their neutral state before hole capture, as shown in Fig. 4(a) (top), while they relax asymmetrically once they have captured a hole (bottom). Several electron paramagnetic resonance studies have shown that the densities of these positively charged defects correlate with the density of oxide trapped holes, confirming the physical origin of the hole traps, as shown in Fig. 4(b) [28]-[29].

D. *Interface traps generation*

In addition to the capture of holes in traps within the oxide, radiation also causes an increase in the density of traps at the Si/SiO_2 interface. Several electron spin resonance studies have concluded that interface traps are associated with a defect known as a P_b center, in which a silicon atom forming three bonds with oxygen atoms has the fourth bond unformed, a phenomenon known as a *dangling bond* [30]-[31]. This type of defect is due to the imperfect oxidation of the substrate, resulting in an allowed electronic state within the semiconductor bandgap. Because they are located at the interface, these traps can exchange charge with the semiconductor bands, making their charge state dependent on the applied bias. During the fabrication process, these traps are passivated by annealing in a hydrogen-rich environment, leading to the formation of a Si-H bond that eliminates the electronic state within the bandgap.

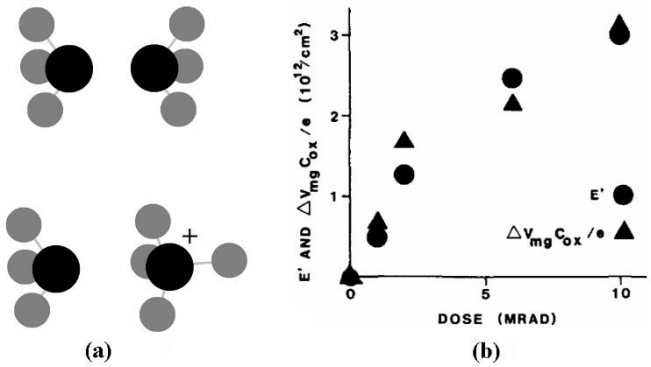

Fig. 4. (a) Oxygen vacancy before (top) and after (bottom) hole trapping. (Silicon atoms are in black, oxygen atoms are in gray), and (b) Densities of trapped holes and positively charged oxygen vacancies as a function of dose [28].

The physical origin of interface traps generation during irradiation is due to a series of processes involving hydrogen. First, after hole capture within the oxide, some of the traps involved are hydrogenated, leading to the subsequent emission of a hydrogen proton (H^+) from them. Depending on the electric field, this proton is drifted towards the interface with the substrate, where it interacts with a Si-H center, depassivating it and consequently generating an interface trap [32]-[33]. Figure 5 shows the dependence of interface traps generation on the applied electric field. Curve A and E correspond to experiments performed under a positive and a negative electric field throughout the entire time, respectively. A positive electric field favors interface traps generation until saturation is reached, whereas a negative electric field suppresses it. For curves B, C, and D, a positive electric field was applied during the 0.1 s irradiation and throughout the first 0.7 s of post-irradiation. The electric field was then reversed and restored to a positive value after 20, 200, and 2000 s for B, C, and D, respectively. As shown, interface traps generation is completely halted while the electric field is negative and resumes only after the field is switched back to positive. Notably, interface traps generation saturates after approximately 2000 s. Therefore, in curve D, where the electric field is restored to a positive value only after this time, no additional interface traps generation is observed.

E. *Effects on device characteristics*

The main radiation effect on MOS devices is the shift of the transfer characteristic curve I_{DS}-V_{GS} as a consequence of hole capture within the oxide and interface traps generation, which is represented by the variation of threshold voltage according to the following expression

$$\Delta V_t = -\frac{q}{\varepsilon_{ox}}\int_0^{t_{ox}} p_t(t_{ox}-x)dx - \frac{q}{C_{ox}}N_{it}$$

where q is the elementary charge, ε_{ox} is the SiO_2 permittivity, t_{ox} is the oxide thickness, x is the distance from the Si/SiO_2 interface, C_{ox} is the oxide capacitance, p_t is the density of trapped holes, and N_{it} is the density of interface traps positively charged at threshold condition.

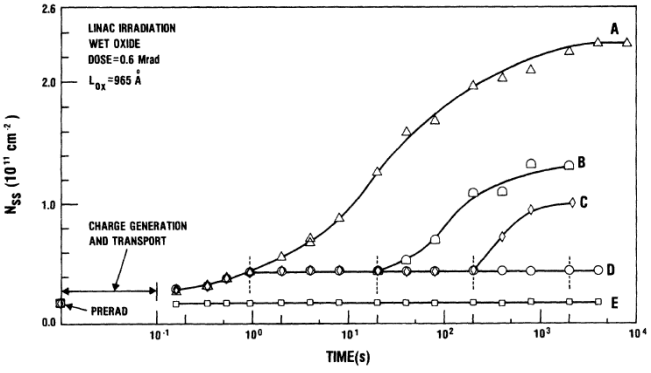

Fig. 5. Dependence of interface traps generation on the applied electric field for experiments where the electric field is reversed and restored at different times after irradiation [32].

elektron
Revista Elektron, Vol. 10, No. 1, pp. 12–24 (2026)
https://doi.org/10.37537/rev.elektron.10.1.237.2026
Review Article

Since the charge density in interface traps depends on the position of the Fermi level within the bandgap, this means that the induced V_t-shift is not constant but depends on the applied bias. Consequently, the increase in interface traps density generates a change in the slope of the curve in the subthreshold region. Figure 6 shows the evolution of the transfer curve for different absorbed doses, where both the shift of the entire curve and the change in its subthreshold slope can be observed. Unlike the contribution due to holes trapped within the oxide, the charge in interface traps at threshold is positive for p-channel transistors, while it is negative for n-channel transistors. This means that the V_t-shift in the latter has two opposing contributions, making the evolution potentially non-monotonic.

Interface traps generation also modifies the transfer curve because it reduces the mobility of the carriers in the channel, as a consequence of the Coulomb interaction between them and the charge in the traps, as shown in Fig. 7, where the evolution with dose and time after radiation of the current factor k (proportional to the mobility μ) and the interface traps density N_{it} is observed [34].

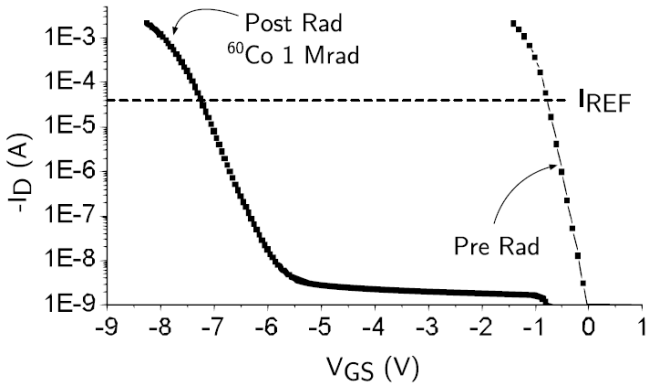

Fig. 6. Transfer characteristic I_{DS}-V_{GS} of a p-channel MOSFET before and after γ-ray (^{60}Co) 1 Mrad irradiation.

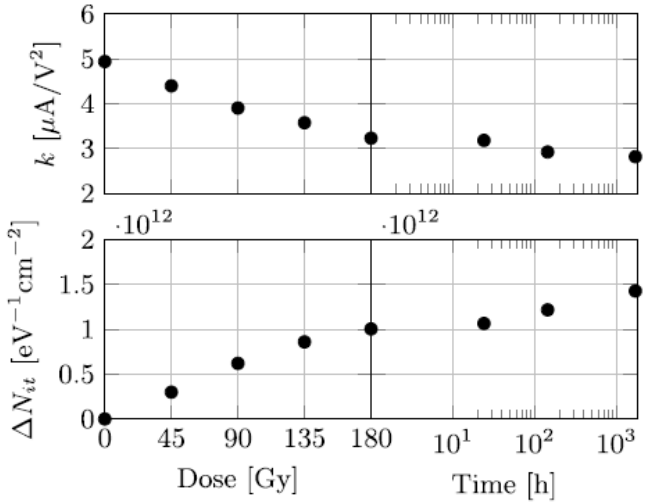

Fig. 7. Evolution of k (proportional to mobility μ) and interface traps density N_{it} as a function of absorbed dose and the time after irradiation ends [34].

Ionizing radiation also leads to an increase in *flicker noise*, characterized by a power spectral density proportional to *1/f*, where *f* is the signal frequency. Its physical origin is due to fluctuations in the number of carriers in the channel as a consequence of tunneling transitions between the channel and the traps within the oxide. It has been observed that the noise power correlates very well with the V_t-shift due to hole capture and emission within the oxide during irradiation and subsequent annealing, respectively [35]-[37], as shown in Fig. 8.

For sufficiently thin oxides, radiation causes an increase in the leakage current across the gate oxide as a consequence of an inelastic tunneling process at low/medium electric fields involving traps within the oxide, as has been observed for different radiation sources, including γ rays (^{60}Co) [38], electrons, X-rays, and ions [39]-[40]. Similar to what is observed for the noise, the increase in leakage current is strongly correlated with the density of holes trapped within the oxide during irradiation [41].

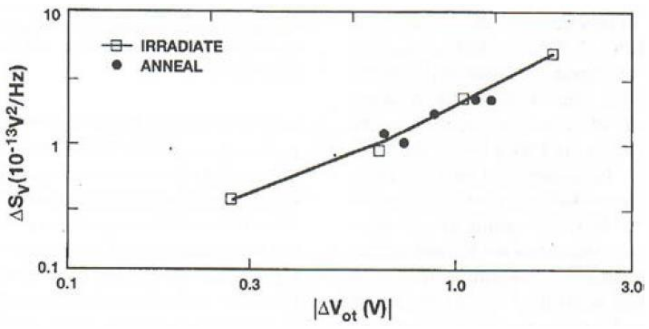

Fig. 8. Noise power as a function of threshold voltage shift induced by trapped holes [36].

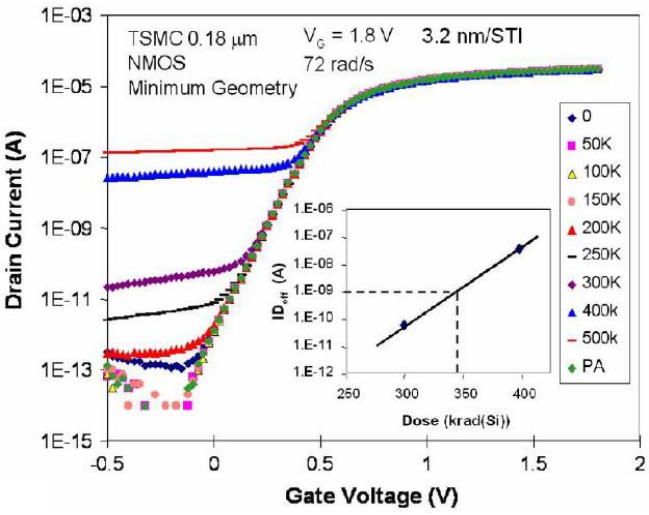

Fig. 9. Transfer characteristic I_{DS}-V_{GS} of a 0.18 μm n-channel MOSFET for different absorbed doses [42].

elektron
Revista Elektron, Vol. 10, No. 1, pp. 12–24 (2026)
https://doi.org/10.37537/rev.elektron.10.1.237.2026
Review Article

As the oxide thickness decreases, the effect of the V_t-shift gradually diminishes, and the hole capture within the field oxides used to isolate adjacent devices becomes dominant for the radiation effects on MOS devices. Since this oxide is not grown with the same care as gate oxides, its radiation response can be highly variable. Even if its response were comparable to that of gate oxides, the trapped charge density is much higher in field oxides because they are thicker. Hole capture in these oxides leads to an increase in standby current as a consequence of parasitic conduction paths [42], as shown in Fig. 9.

III. MOS Dosimeter

The MOS dosimeter was first proposed by Poch and Holmes-Siedle in 1970 [43], and later refined by Holmes-Siedle [44] for sensing radiation in space by tracking the V_t-shift, leading to the commercial MOS dosimeter known as RADFET [45]-[49]. To estimate absorbed dose, each dosimeter must be calibrated as dispersion of 5% was common [50]-[51], reaching 16% for thicker oxides [52].

The standard measurement setup consists of irradiating the device with all its terminals short-circuited and measuring V_t before and after irradiation, as shown in Fig. 10(a), where the definition of V_t is taken as the gate-to-source voltage corresponding to a predefined reference drain-to-source current I_{REF}. In order to increase its radiation sensitivity, it is possible to apply a bias voltage to the gate during irradiation, as shown in Fig. 10(b). Real-time measurements are possible if both configurations are switched, with the device lying mostly in biasing mode and reading V_t periodically.

Over the years, various commercial MOS dosimeters have appeared. Table I gives information about some of them, considering those that have oxide thickness in the range 300-500 nm to facilitate comparison. RADFET from REM Oxford includes different dosimeters with oxide thickness ranging from 120 nm up to 1.23 μm, which allows to calibrate the sensitivity, with good linearity range up to 10 Gy, and low fading of less than one percent after ten days [53].

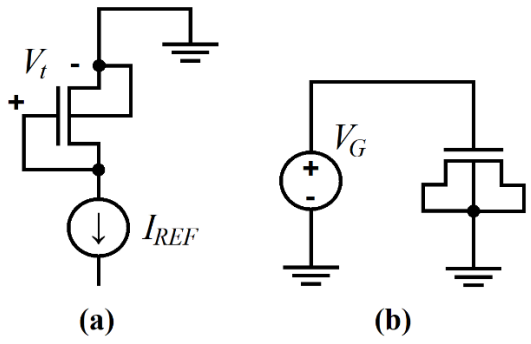

Fig. 10. Simplified schematics of the measurement setup at (a) reading mode, and (b) biasing mode.

In addition to a standard dosimeter [54]-[55], Best Medical offers different types of dosimeters depending on the application, such as the microMOSFET that fits in a 6 Fr catheter and can be used to monitor the dose in brachytherapy treatments [56], as well as the Linear 5ive Array that allows monitoring the dose at different points for in vivo dosimetry or beam quality assurance [57]. Varadis presents dosimeters with nonlinear responses, whose reading uses a calibration curve for the batch, and a dynamic range between 1 cGy and 1 kGy for an oxide thickness of 400 nm, and between 3 mGy and 10 Gy for an oxide thickness of 1 μm [58]. MOSkin is a dosimeter specially developed to be used in radiotherapy treatments [59], showing very good linearity even for ultra-high dose rate regime up to 35 Gy with 200 ns radiation pulses with instantaneous dose rates as high as 2×10^9 Gy/s [60]. The OneDose was a disposable dosimeter designed for single use [61], widely employed during the 2000s [62]-[63], although later discontinued.

TABLE I
Commercial Dosimeters

Dosimeter	t_{ox} [nm]	V_G [V]	S [mV/Gy]
REM Oxford RFT300 [53]	300	0 / 9	20 / 125
Best Medical 502RD [54]-[55]	500	5 / 15	100 / 300
Varadis VT01 [58]	400	0	65
MOSkin [59]	550	12	250
OneDose [61]	400	0	35-100

A. *Temperature-induced errors*

Temperature variations affect the MOSFET transfer characteristic due to two combined effects: a shift in the threshold voltage and a decrease in carriers' mobility [51]. If the temperature is not controlled during dosimeter readings, the temperature-induced V_t-shift can be misinterpreted as being due to the presence of radiation, leading to an error in the dosimeter reading. In addition to control the temperature when the dosimeter is read [64], there are three possibilities to mitigate this type of error. First, if the effect of temperature on V_t is characterized, it is possible to read the temperature during the acquisition of V_t and apply a correction that subtracts the V_t-shift induced by temperature variations. Secondly, the transfer curve has a current value at which the voltage value V_{GS} is independent of temperature, which is called the zero-temperature coefficient current (I_{ZTC}). If the reference current at which V_t is read is set to I_{ZTC}, temperature errors are expected to be significantly reduced, as shown in Fig. 11(a). However, the two previous options assume that the effects of temperature on the device characteristics are stable, i.e., that they do not change as the absorbed dose increases, but this has been experimentally shown not to be the case [52], [64]-[65]. For example, Fig. 11(b) shows how I_{ZTC} changes due to irradiation, making the value of V_t sensitive to temperature again, unless the current I_{ZTC} is corrected during irradiation.

elektron
Revista Elektron, Vol. 10, No. 1, pp. 12–24 (2026)
https://doi.org/10.37537/rev.elektron.10.1.237.2026

Review Article

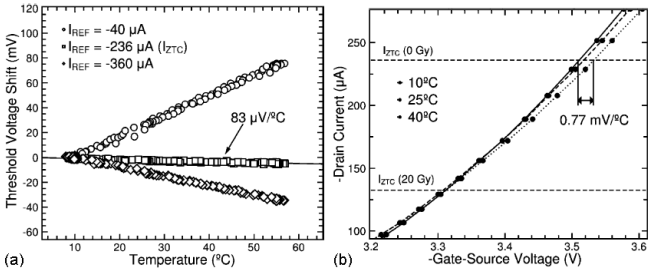

Fig. 11. (a) V_t-shift with temperature for three different currents, and (b) Transfer curve after 20 Gy of absorbed dose and three different temperatures [65].

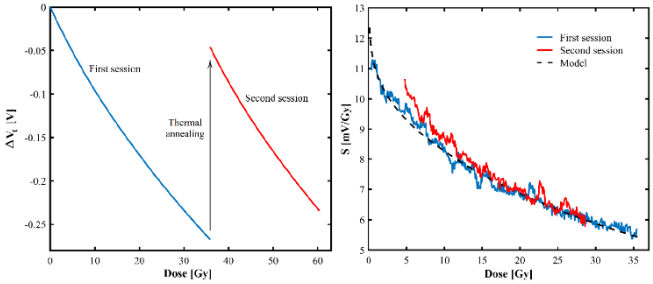

Fig. 12. (a) Threshold voltage and (b) sensitivity evolutions during two consecutive irradiations with a thermal annealing treatment between them [76].

A third alternative is to use two matched dosimeters, instead of just one, and take a differential reading having been biased differently during irradiation, causing their V_t values to evolve differently [66]-[69].

B. Saturation and reutilization

As the absorbed dose increases, the V_t-shift gradually saturates and the dosimeter loses sensitivity. This saturation is due to three different physical mechanisms [70]. First, the finite number of trapping sites establishes a maximum V_t-shift when all the traps are filled. Second, when the density of trapped holes is high enough to distort the local electric field, a process known as *field collapse* occurs, in which the electric field decreases in the oxide region where most of the holes are generated, leading to a lower fractional yield, so there are fewer holes available to be trapped. Third, when the density of trapped holes is sufficiently high, their neutralization by an electron travelling through the oxide is no longer negligible, resulting in a dynamic equilibrium when hole capture is balanced by neutralization.

Different methods were proposed for erasing the charge accumulated during irradiation and restore the dosimeter to its initial state or, at least, to a repeatable predefined state. One technique is based on a high temperature annealing. The exposure to high temperatures leads to a recovery of V_t towards its pre-irradiation value due to the emission of holes from traps to the valence band of the oxide and their subsequent transport towards either electrode [71], so different groups propose to use thermal annealing as a way for reusing the MOS dosimeter [72]-[76]. Figure 12 shows the procedure for a dosimeter exposed up to 400 °C for half an hour, achieving good repeatability [76]. Alternatively, illuminating with UV light also anneals the charge within the oxide due to the electron injection of electrons from the substrate into the oxide conduction band by overcoming the barrier energy at the interface, which leads to the proposal of using UV exposure for dosimeter reuse [74]. It was also reported that local reheating by electric current also anneals the charge within the oxide [77]-[78].

Another possibility is related to applying a high external electric field making possible the injection of electrons from the substrate into the oxide conduction band by means of Fowler-Nordheim (FN) tunneling. These injected electrons produce impact ionization and the capture of some of the generated holes, while the electrons can recombine with positively charged traps. A steady state is reached as a result of a dynamic balance between the two processes, which depends on the electric field applied during injection or the current in the case of constant-current injection [79]-[82]. Interface traps are also generated during electron injection until the process saturates at a high enough charge density around 0.1 C/cm^2 is injected [79]. It was observed that this mechanism allows to set V_t to a predefined value, even when the MOS device was previously irradiated, so it can be used for the erasure of the radiation-induced oxide charge. Thus, the proposed technique consists of a preparation for setting V_t to a chosen value and saturating interface traps density. Then, the dosimeter is ready for use. After irradiation, the injection process is employed to reset V_t to the same initial value, making the dosimeter reusable again. The use of this technique allows to obtain a dispersion smaller than 2% after many irradiation-erasure cycles reaching a total absorbed dose around 50 kGy [83]. The technique was also tested for commercial RADFET with good results [84], as shown in Fig. 13.

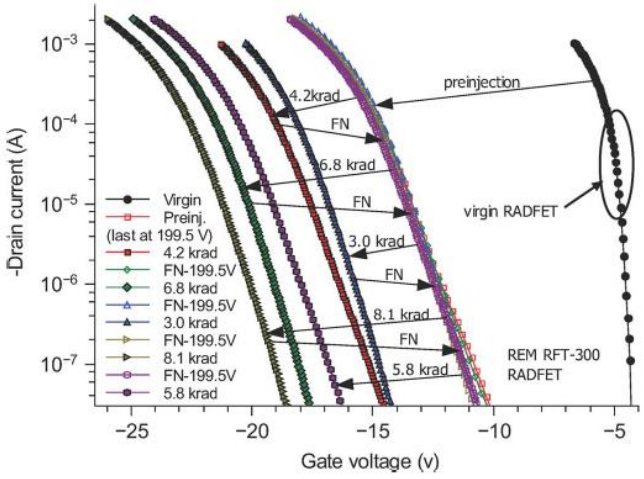

Fig. 13. I_{DS}-V_{GS} curves for a RADFET subjected to many cycles of irradiation and electrically erasure [84].

elektron
Revista Elektron, Vol. 10, No. 1, pp. 12–24 (2026)
https://doi.org/10.37537/rev.elektron.10.1.237.2026

Review Article

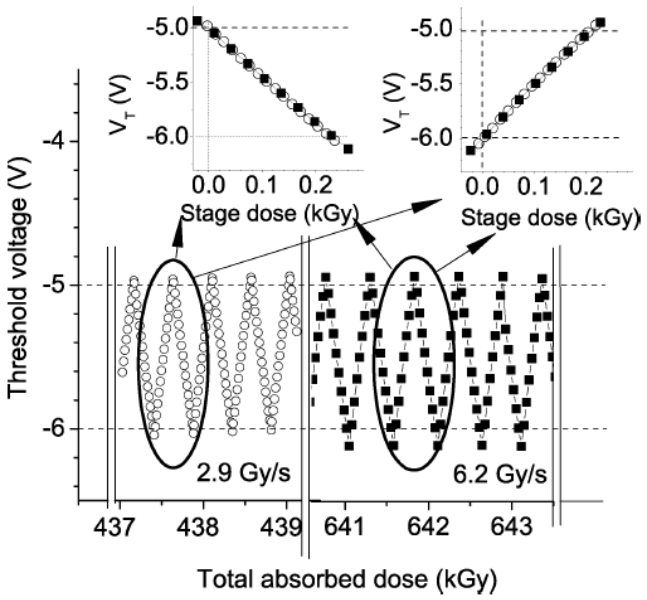

Fig. 14. Threshold voltage evolution with dose during two parts of a long irradiation under BCCM, showing excellent repeatability [86].

For real-time measurements, it is also possible to extend the measurement range taking advantage of charge neutralization. As previously discussed, when a positive bias is applied during irradiation, holes are trapped within oxide, which is also known as positive charge buildup (PCB). If after a certain absorbed dose, the bias is switched to a negative value, the oxide electric field is reversed, so the radiation-generated electrons move towards the interface with the substrate, where most of the trapped holes are located, leading to an increase in the neutralization rate and a recovery of V_t, which is known as radiation-induced charge neutralization (RICN) [85]. If both PCB and RICN stages are repeated alternately, it is possible to keep V_t within a predefined window, maintaining a constant sensitivity and extending the measurement range, which is dubbed as the bias-controlled cycled measurement (BCCM) technique [86]. After interface traps saturation, which occurs around tens of kGy, the response is repeatable between cycles, as shown in Fig. 14, where the response of a dosimeter for two parts of a prolonged irradiation is observed, which, although separated by ~200 kGy, overlap within measurement error. This measurement technique has additional advantages, as measurement uncertainties even lower than the dispersion in the responses among different devices, and a reduction by a factor of ten of the temperature-induced dose error when temperature changes over a range between -5 °C and 95 °C [87]. The technique was also applied to commercial RADFET [84], validating the results.

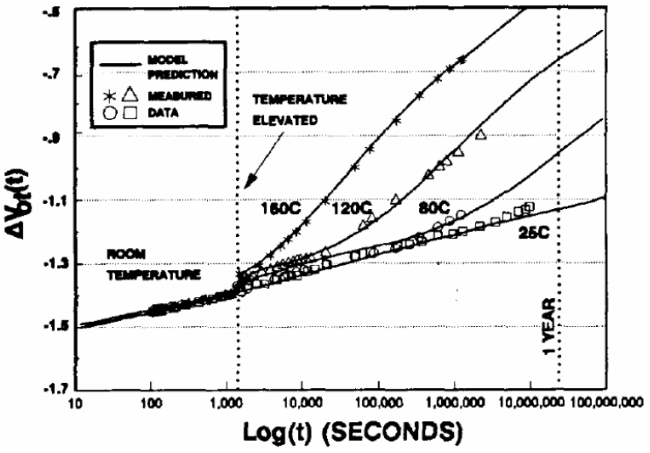

Fig. 15. Recovery of threshold voltage as a function of the time after irradiation ends for different temperatures [88].

C. Post-irradiation stability

For a MOS dosimeter to be considered suitable, it must retain information for a sufficiently long time, which is directly related with the stability of the charge trapped within the oxide. Once irradiation ends, the density of trapped holes gradually decreases, a phenomenon known as *annealing*, which is a consequence of the neutralization induced by either tunnel transitions between the substrate and the traps and the emission of holes from the traps to the valence band [88]. Given the exponential dependence of tunneling probability on distance and of thermal emission probability on energy, the observed post-radiation recovery is associated with the presence of a spatial and energetic distribution of trapped holes within the oxide. Annealing exhibits a dynamic approximately linear with *log(t)* and is highly dependent on applied bias and temperature, due to the dependence of tunneling probability and thermal emission on these parameters, respectively. Figure 15 shows the threshold voltage recovery as a function of post-radiation time for different temperatures.

D. FOXFET

In order to increase the sensor sensitivity, MOS dosimeters require thick gate oxides [89]-[91], which goes in the opposite direction to the technology trend for scaling down dimensions, so they are usually fabricated in ad-hoc processes, increasing their cost, compromising their reliability, and making it more difficult to integrate with the reading circuit. To overcome this issue, it was proposed to use the field oxide commonly used as passivation as the gate oxide of a high sensitivity dosimeter, the FOXFET [92], as in the cross-section shown in Fig. 16. Field oxides are known to be sensitive to radiation and responsible for an increase in leakage current after irradiation [93]-[95]. FOXFET dosimeters from two different processes were fabricated and both showed a response comparable to commercial MOS dosimeters (Fig. 17) [92], suitable for in vivo dosimetry in radiotherapy [96].

elektron
Revista Elektron, Vol. 10, No. 1, pp. 12–24 (2026)
https://doi.org/10.37537/rev.elektron.10.1.237.2026

Review Article

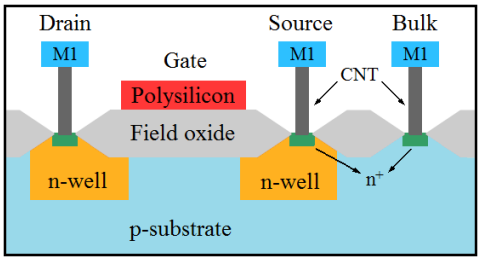

Fig. 16. Cross section of the FOXFET dosimeter.

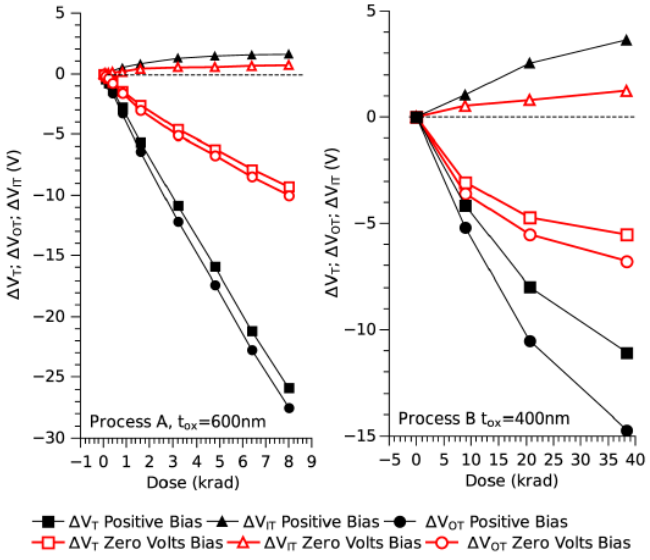

Fig. 17. Total threshold voltage and the contributions due to oxide and interface traps as a function of absorbed dose for FOXFET fabricated in two different CMOS processes [92].

IV. Floating Gate Dosimeter

The floating gate (FG) MOSFET is a transistor where an oxide is over the gate, leaving it isolated from external electrical connection, i.e., floating. When a second polysilicon layer is deposited onto the top oxide, this can be employed as control gate (CG) and the FG-MOSFET is akin any other MOSFET. Given that the presence of the oxides surrounding the FG makes the structure sensitive to radiation, it was proposed to employ that as a dosimeter [97]. The basic idea involves a floating gate, initially charged with electrons, which is irradiated with zero bias in the CG, as shown in the band diagram of Fig. 18. The electrons in the FG generate the necessary electric field in the oxides, allowing the electron-hole pairs generated by the radiation to escape from the initial recombination. The direction of these electric fields favours the electrons to left the oxide, while the holes are attracted to the FG, where they recombine with the electrons already present, leading to a measurable V_t-shift. Thus, dosimeters based on FG structures do not rely on the hole capture in traps within the oxide, but rather on recombination with the charge present in a polysilicon layer. However, it would still be possible to consider that both types of devices operate under a common principle if we view the floating gate as a kind of large sheet of traps in the middle of the oxide.

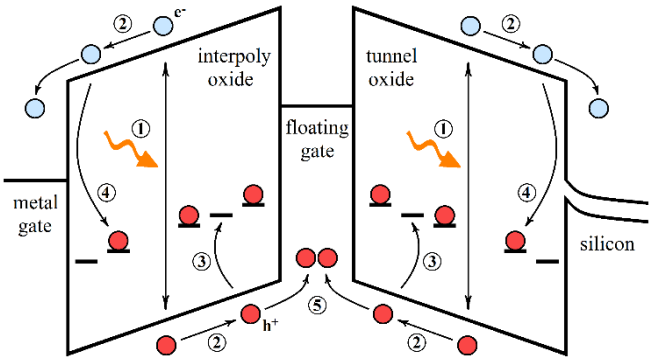

Fig. 18. Band diagram schematic representation of the irradiation of a floating gate structure with zero applied bias and negative charge initially at the floating gate. ① charge generation and initial recombination, ② electron (blue) and hole (red) transport, ③ hole trapping, ④ trapped hole neutralization through electron trapping, and ⑤ charge injection into the floating gate.

Furthermore, the initial charge on the FG allows an electric field to exist in the oxides, increasing sensitivity without the need for an external connection that applies a voltage to the CG, which is advantageous for applications where a wired connection is undesirable.

A notable improvement involved extending the floating gate over the field oxide (Fig. 19(a)) to take advantage of its larger ionization volume, thereby increasing the sensor sensitivity [98]. In that initial work, the electric field in the field oxide, necessary to maximize the fractional yield, was generated by biasing the CG, but later it was achieved by pre-injecting an initial charge into the FG [99]. As the CG-to-FG capacitance reduces the sensitivity, it was proposed to remove the CG at the cost of a smaller measurement range [100]. A natural way to reuse the FG dosimeter consists of recharged the FG, and the results (Fig. 19(b)) showed a reasonable agreement between first and second irradiation sensitivity as a function of the threshold voltage for FG dosimeters initially charged with electrons or holes [99].

Temperature variations also affect FG dosimeters due to changes in threshold voltage and carrier mobility [101], so a differential technique and also a compensation method were employed to mitigate that [100]. For FG dosimeters with a CG, a way to extend the measurement range is to apply the BCCM technique discussed in section III.B, which shows that it is possible to keep a roughly constant sensitivity with good repeatability across successive cycles [102].

The FG sensor is the core of many different proposals for MOS dosimeters in recent years [103]-[109]. It was also proposed to use an ultraviolet erasable programmed read-only memory as a dosimeter, given that the number of memory cells that flips from “0” to “1” state is a linear or power-law function of the absorbed dose [110]-[112]. Some groups also employed commercial FG devices as MOS dosimeters [113]-[115].

elektron
Revista Elektron, Vol. 10, No. 1, pp. 12–24 (2026)
https://doi.org/10.37537/rev.elektron.10.1.237.2026

Review Article

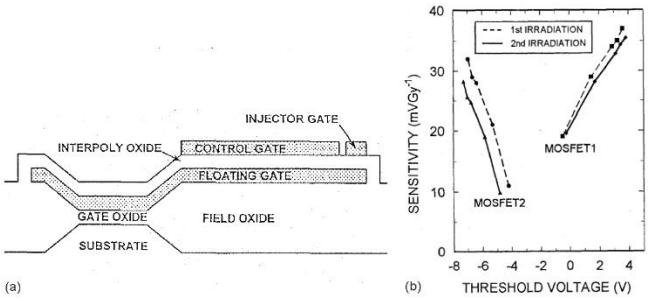

Fig. 19. (a) Cross-section of a floating gate dosimeter with extension over field oxide, and (b) sensitivity as a function of the threshold voltage for FG dosimeters initially charge with electrons (MOSFET1) or holes (MOSFET2) during the first and second irradiations [99].

As a summary, Table II shows the main characteristics of some of the different proposals based on FG structures. As noted, the different proposed dosimeters do not use the same kind of dosimetric signal, since some of them indirectly measure the voltage at the floating gate [100], [108], while others measure the decrease in drain current as the floating gate discharges, either directly [104] or converted into a proportional frequency signal [107], making a direct comparison between sensitivities difficult. What can be directly compared is the so-called temperature error factor, since this is calculated as the ratio between the temperature and radiation sensitivities, making it independent of the type of signal being measured. The same applies to the noise equivalent dose (NED), which represents the sensor's resolution in terms of the noise-induced dose reading error. Although the dosimeter proposed in [108] appears to have the best characteristics, it has the disadvantage of a dose range of only 2.8 Gy, compared to the three remaining ones that all have ranges above 10 Gy.

TABLE II
FLOATING GATE DOSIMETERS

Ref.	t_{fox}	S_R	*TEF*	*NED*
[100]	1 µm	300 mV/Gy	270 mGy/°C	5 mGy
[104]	N/A	1.14 µA/Gy	54.3 mGy/°C	19 mGy
[107]	N/A	34.7 kHz/Gy	3.9 mGy/°C	0.16 mGy
[108]	350 nm	386 mV/Gy	0.94 mGy/°C	0.5 mGy

One area where FG dosimeters could potentially outperform conventional MOS dosimeters is in data retention, as the data is stored in an electrically isolated layer. However, FG dosimeters have also been reported to exhibit fading [107]. To determine the source of this charge loss, non-irradiated structures were charged, and it was verified that the charge on the FG remained stable. Consequently, it was concluded that the observed annealing is related to the neutralization of holes captured in the tunnel oxide.

V. CONCLUSIONS

This work provides a review of radiation effects in MOS devices, with a focus on MOS dosimetry for space and medical applications. We begin by describing the microscopic processes that leads to the positive charge formation within the gate oxide and the generation of traps at the substrate/oxide interface, including electron-hole pair generation and initial recombination, carrier transport, hole capture in oxide traps, proton release, transport, and reaction at the interface, depassivating a dangling bond. Next, we describe how the effects of radiation on MOS devices can be harnessed to measure absorbed dose, leading to MOS dosimetry. We present the standard method of operation and reading, and then discuss the main limitations of this type of sensor, such as its temperature dependence, limited measurement range, and information retention, outlining the ways in which these limitations are typically addressed. Finally, we analyze the feasibility of using a floating-gate structure as a dosimeter. By pre-injecting charge into the floating gate, the dosimeter can achieve high sensitivity while operating under zero-bias conditions.

ACKNOWLEDGMENT

This work was supported by the Universidad de Buenos under grants UBACYT 20020220400105BA and 20020220300077BA; and by the Agencia Nacional de Promoción de la Investigación, el Desarrollo Tecnológico y la Innovación under grant PICT 2020-A-01957.

DATA AVAILABILITY STATEMENT

As a review article, there is no data that can be shared.

CREDIT AUTHORSHIP CONTRIBUTION STATEMENT

L. Sambuco Salomone: Conceptualization, Investigation, Writing-Original Draft, Writing-Review and Editing. **S. Carbonetto:** Conceptualization, Investigation, Writing-Review and Editing. **M. V. Cassani:** Conceptualization, Investigation, Writing-Review and Editing. **M. A. Garcia-Inza:** Conceptualization, Investigation, Writing-Review and Editing. **E. Redin:** Conceptualization, Supervision. **A. Faigón:** Conceptualization, Project administration.

REFERENCES

[1] J. R. Kopacz, R. Herschitz, and J. Roney, "Small satellites an overview and assessment," *Acta Astronautica*, vol. 170, pp. 93-105, 2020, doi: https://doi.org/10.1016/j.actaastro.2020.01.034.

[2] R. Velazco, D. McMorrow, and J. Estela (Eds.), "Radiation effects on integrated circuits and systems for space applications," Springer, 2019.

[3] J. Mazur, L. Friesen, A. Lin, D. Mabry, N. Katz, Y. Dotan, J. George, J. B. Blake, M. Looper, M. Redding, T. P. O'Brien, J. Cha, A. Birkitt, P. Carranza, M. Lalic, F. Fuentes, R. Galvan, and M. McNab, "The relativistic proton spectrometer (RPS) for the radiation belt storm probes mission," *Space Science Reviews*, vol. 179, pp. 221-261, 2013, doi: https://doi.org/10.1007/s11214-012-9926-9.

[4] J. E. Mazur, T. P. O'Brien, and M. D. Looper, "The relativistic proton spectrometer: A review of sensor performance, applications, and science," *Space Science Reviews*, vol. 219, no. 3, p. 26, 2023, doi: https://doi.org/10.1007/s11214-023-00962-2.

[5] H. Zhao, W. R. Johnston, D. N. Baker, X. Li, B. Ni, A. N. Jaynes, S. G. Kanekal, J. B. Blake, S. G. Claudepierre, G. D. Reeves, and A. J. Boyd, "Characterization and evolution of radiation belt electron energy spectra based on the Van Allen probes measurements,"

Journal of Geophysical Research: Space Physics, vol. 124, pp. 4217-4232, 2019, doi: https://doi.org/10.1029/2019JA026697.

[6] A. W. Strong, E. Orlando, and T. R. Jaffe, "The interstellar cosmic-ray electron spectrum from synchrotron radiation and direct measurements," *Astronomy and Astrophysics*, vol. 354, p. A54, 2011, doi: https://doi.org/10.1051/0004-6361/201116828.

[7] "Comprehensive QA for radiation oncology," American Association of Physicists in Medicine, report N46, 1994.

[8] "In vivo dosimetry," *ASN Patient Safety*, no. 5, 2014.

[9] L. Brualla, M. Rodriguez, J. Sempau, and P. Andreo, "PENELOPE/PRIMO-calculated photon and electron spectra from clinical accelerators," *Radiation Oncology*, vol. 14, no. 1, p. 6, 2019, doi: https://doi.org/10.1186/s13014-018-1186-8.

[10] P. Papagiannis, A. Angelopoulos, E. Pantelis, L. Sakelliou, P. Karaiskos, and Y. Shimizu, "Monte Carlo dosimetry of ^{60}Co HDR brachytherapy sources," *Medical Physics*, vol. 30, no. 4, pp. 712-721, 2003, doi: https://doi.org/10.1118/1.1563662.

[11] R. Nath, L. L. Anderson, G. Luxton, K. A. Weaver, J. F. Williamson, and A. S. Meigooni, "Dosimetry of interstitial brachytherapy sources: Recommendations of the AAPM Radiation Therapy Committee Task Group No. 43," *Medical Physics*, vol. 22, no. 2, pp. 209-234, 1995, doi: https://doi.org/10.1118/1.597458.

[12] R. Mohan, "A review of proton therapy – Current status and future prospects," *Precision Radiation Oncology*, vol. 6, no. 2, pp. 164-176, 2022, doi: https://doi.org/10.1002/pro6.1149.

[13] G. A. Ausman, and F. B. McLean, "Electron-hole pair creation in SiO_2," *Harry Diamond Laboratories Technical Report*, HDL-TR-1720, 1975.

[14] J. M. Benedetto, and H. E. Boesch, "The relationship between ^{60}Co and 10-keV X-ray damage in MOS devices," *IEEE Transactions on Nuclear Science*, vol. 33, no. 6, pp. 1318-1323, 1986, doi: https://doi.org/10.1109/TNS.1986.4334599.

[15] T. R. Oldham, and J. M. McGarrity, "Ionization of SiO_2 by heavy charged particles," *IEEE Transactions on Nuclear Science*, vol. 28, no. 6, pp. 3975-3980, 1981, doi: https://doi.org/10.1109/TNS.1981.4335658.

[16] T. R. Oldham, "Recombination along the tracks of heavy charged particles in SiO_2 films," *Journal of Applied Physics*, vol. 57, no. 8, pp. 2695-2702, 1985, doi: https://doi.org/10.1063/1.335409.

[17] H. E. Boesch, and J. M. McGarrity, "Charge yield and dose effects in MOS capacitors at 80 K," *IEEE Transactions on Nuclear Science*, vol. 23, no. 6, pp. 1520-1525, 1976, doi: https://doi.org/10.1109/TNS.1976.4328532.

[18] T. R. Oldham, and J. M. McGarrity, "Comparison of 60Co response and 10 keV X-ray response in MOS capacitors," *IEEE Transactions on Nuclear Science*, vol. 30, no. 6, pp. 4377-4381, 1983, doi: https://doi.org/10.1109/TNS.1983.4333141.

[19] F. B. McLean, and T. R. Oldham, "Basic mechanisms of radiation effects in electronic materials and devices," *Harry Diamond Laboratory, Tech. Rep.*, HDL-TR-2129.

[20] C. M. Dozier, D. M. Fleetwood, D. B. Brown, and P. S. Winokur, "An evaluation of low-energy X-ray and cobalt-60 irradiations of MOS transistors," *IEEE Transactions on Nuclear Science*, vol. 34, no. 6, pp. 1535-1539, 1987, doi: https://doi.org/10.1109/TNS.1987.4337511.

[21] R. J. Krantz, L. W. Aukerman, and T. C. Zietlow, "Applied field and total dose dependence of trapped charge buildup in MOS devices," *IEEE Transactions on Nuclear Science*, vol. 34, no. 6, pp. 1196-1201, 1987, doi: https://doi.org/10.1109/TNS.1987.4337452.

[22] R. C. Hughes, "Hot electrons in SiO_2," *Physical Review Letters*, vol. 35, no. 7, pp. 449-452, 1975, doi: https://doi.org/10.1103/PhysRevLett.35.449.

[23] M. V. Fischetti, D. J. DiMaria, S. D. Brorson, T. N. Theis, and J. R. Kirtley, "Theory of high-field electron transport in silicon dioxide," *Physical Review B*, vol. 31, no. 12, pp. 8124-8142, 1985, doi: https://doi.org/10.1103/PhysRevB.31.8124.

[24] O. L. Curtis, and J. R. Srour, "The multiple-trapping model and hole transport in SiO_2," *Journal of Applied Physics*, vol. 48, no. 9, pp. 3819-3828, 1977, doi: https://doi.org/10.1063/1.324248.

[25] M. Schaffman, M. Silver, C. Corthell, and R. C. Hughes, "Simulations of the transient photoconductivity in a-SiO_2 using a multiple-trap model," *Journal of Applied Physics*, vol. 51, no. 1, pp. 490-494, 1979, doi: https://doi.org/10.1063/1.327349.

[26] F. B. McLean, H. E. Boesch, and J. M. McGarrity, "Hole transport and recovery characteristics of SiO_2 gate insulators," *IEEE Transactions on Nuclear Science*, vol. 23, no. 6, pp. 1506-1512, 1976, doi: https://doi.org/10.1109/TNS.1976.4328530.

[27] F. B. McLean, H. E. Boesch, and J. M. McGarrity, "Dispersive hole transport in SiO_2," *Harry Diamond Laboratories Report*, HDL-TR-2117, 1987.

[28] P. M. Lenahan, and P. V. Dressendorfer, "Hole traps and trivalent silicon centers in metal/oxide/silicon devices," *Journal of Applied Physics*, vol. 55, no. 10, pp. 3495-3499, 1984, doi: https://doi.org/10.1063/1.332937.

[29] Y. Y. Kim, and P. M. Lenahan, "Electron-spin-resonance study of radiation-induced paramagnetic defects in oxides grown on (100) silicon substrates," *Journal of Applied Physics*, vol. 64, no. 7, pp. 3551-3557, 1988, doi: https://doi.org/10.1063/1.341494.

[30] E. H. Poindexter, P. Caplan, B. E. Deal, and R. R. Razouk, "Interface states and electron spin resonance centers in thermally oxidized (111) and (100) silicon wafers," *Journal of Applied Physics*, vol. 52, no. 2, pp. 879-884, 1981, doi: https://doi.org/10.1063/1.328771.

[31] P. M. Lenahan, K. L. Brower, and P. V. Dressendorfer, "Radiation-induced trivalent silicon defect buildup at the Si-SiO_2 interface in MOS structures," *IEEE Transactions on Nuclear Science*, vol. 28, no. 6, pp. 4105-4106, 1981, doi: https://doi.org/10.1109/TNS.1981.4335683.

[32] F. B. McLean, "A framework for understanding radiation-induced interface states in SiO_2 MOS structures," *IEEE Transactions on Nuclear Science*, vol. 27, no. 6, pp. 1651-1657, 1980, doi: https://doi.org/10.1109/TNS.1980.4331084.

[33] M. R. Shaneyfelt, J. R. Schwank, D. M. Fleetwood, P. S. Winokur, K. L. Hughes, and F. W. Sexton, "Field dependence of interface-trap buildup in polysilicon and metal gate MOS devices," *IEEE Transactions on Nuclear Science*, vol. 37, no. 6, pp. 1632-1640, 1990, doi: https://doi.org/10.1109/23.101171.

[34] R. García Cozzi, E. Redín, M. Garcia-Inza, L. Sambuco Salomone, A. Faigón, S. Carbonetto, "Influence of interface traps on MOSFETs thermal coefficients and its effects on the ZTC current," *Microelectronics Reliability*, vol. 137, 114752, 2022, doi: https://doi.org/10.1016/j.microrel.2022.114752.

[35] D. M. Fleetwood, and J. H. Scofield, "Evidence that similar point defects cause 1/f noise and radiation-induced-hole trapping in metal-oxide-semiconductor transistors," *IEEE Transactions on Nuclear Science*, vol. 64, no. 5, pp. 579-582, 1990, doi: https://doi.org/10.1103/PhysRevLett.64.579.

[36] T. L. Meisenheimer, and D. M. Fleetwood, "Effect of radiation-induced charge on 1/f noise in MOS devices," *IEEE Transactions on Nuclear Science*, vol. 37, no. 6, pp. 1696-1702, 1990, doi: https://doi.org/10.1109/23.101179.

[37] T. L. Meisenheimer, D. M. Fleetwood, M. R. Shaneyfelt, and L. C. Riewe, "1/f noise in n- and p-channel MOS devices through irradiation and annealing," *IEEE Transactions on Nuclear Science*, vol. 38, no. 6, pp. 1297-1303, 1991, doi: https://doi.org/10.1109/23.124108 .

[38] A. Scarpa, A. Paccagnella, F. Montera, G. Ghibaudo, G. Pananakakis, G. Ghidini, and P. G. Fuochi, "Ionizing radiation induced leakage current on ultra-thin gate oxides," *IEEE Transactions on Nuclear Science*, vol. 44, no. 6, pp. 1818-1825, 1997, doi: https://doi.org/10.1109/23.658948.

[39] M. Ceschia, A. Paccagnella, A. Cester, A. Scarpa, and G. Ghidini, "Radiation induced leakage current and stress induced leakage current in ultra-thin gate oxides," *IEEE Transactions on Nuclear Science*, vol. 45, no. 6, pp. 2375-2382, 1998, doi: https://doi.org/10.1109/23.736457.

[40] M. Ceschia, A. Paccagnella, M. Turrini, A. Candelori, G. Ghidini, and J. Wyss, "Heavy ion irradiation of thin gate oxides," *IEEE Transactions on Nuclear Science*, vol. 47, no. 6, pp. 2648-2655, 2000, doi: https://doi.org/10.1109/23.903821.

[41] P. M. Lenahan, J. P. Campbell, A. Y. Kang, S. T. Liu, and R. A. Weimer, "Radiation-induced leakage currents: Atomic scale

mechanisms," *IEEE Transactions on Nuclear Science*, vol. 48, no. 6, pp. 2101-2106, 2001, doi: https://doi.org/10.1109/23.983179.
[42] R. C. Lacoe, "CMOS scaling design principles and hardening by design methodology,"*NSREC Shrot Course*, 2003.
[43] W. J. Poch, and A. G. Holmes-Siedle, "The mosimeter: A new instrument for measuring radiation dose," *RCA Engineer*, vol. 16, no. 3, pp. 56-59, 1970.
[44] A. Holmes-Siedle, "The space-charge dosimeter: General principles of a new method of radiation detection," *Nuclear Instruments and Methods*, vol. 121, no. 1, pp. 169-179, 1974 doi: https://doi.org/10.1016/0029-554X(74)90153-0.
[45] A. Holmes-Siedle, L. Adams, J. S. Leffler, and S. R. Lindgren, "The RADFET system for real-time dosimeter in nuclear facility," *IEEE Transactions on Nuclear Science*, vol. 26, 025004, 1983.
[46] A. G. Holmes-Siedle, L. Adams, B. Pauly, and S. Marsden, "Linearity of pMOS radiation dosimeters operated at zero bias," *Electronics Letters*, vol. 21, no. 3, pp. 570-571, 1985, doi: https://doi.org/10.1049/el:19850403.
[47] A. Holmes-Siedle, and L. Adams, "RADFET: A review of the use of metal-oxide-silicon devices as integrating dosimeters," *Radiation Physics and Chemistry*, vol. 28, no. 2, pp. 235-244, 1986, doi: https://doi.org/10.1016/1359-0197(86)90134-7.
[48] F. Ravotti, M. Glaser, M. Moll, C. Ilgner, B. Camanzi, and A. G. Holmes-Siedle, "Response of RadFET dosimeters to high fluence of fast neutrons," *IEEE Transactions on Nuclear Science*, vol. 52, no. 4, pp. 959-965, 2005, doi: https://doi.org/10.1109/TNS.2005.852709.
[49] A. Holmes-Siedle, F. Ravotti, and M. Glaser, "The dosimetric performance of RADFETs in radiation test beams," *IEEE Radiation Effects Data Workshop*, pp. 42-57, 2007, doi: https://doi.org/10.1109/REDW.2007.4342539.
[50] F. Vettese, C. Donichak, P. Bourgeault, and G. Sarrabayrouse, "Assessment of a new p-MOSFET usable as a dose rate insensitive gamma dose sensor," *IEEE Transactions on Nuclear Science*, vol. 43, no. 3, pp. 991-996, 1996, doi: https://doi.org/10.1109/23.510745.
[51] L. J. Asensio, M. A. Carvajal, J. A. López-Villanueva, M. Vilches, A. M. Lallena, and A. J. Palma, "Evaluation of a low-cost commercial MOSFET as a radiation dosimeter," *Sensors and Actuators A*, vol. 125, pp. 288-295, 2006, doi: https://doi.org/10.1016/j.sna.2005.08.020.
[52] A. Haran, A. Jaksić, N. Refaeli, A. Eliyahu, D. David, and J. Barak, "Temperature effects and long term fading of implanted and unimplanted gate oxide RADFETs," *IEEE Transactions on Nuclear Science*, vol. 51, no. 5, pp. 2917-2921, 2004, doi: https://doi.org/10.1109/TNS.2004.835065.
[53] RFT300-CC10G1 Datasheet (RFTDAT-CC10 - Rev W), REM Oxford Ltd., 2010.
[54] G. Pablo Cirrone, G. Cuttone, P. A. Lojacono, S. L. Nigro, I. V. Patti, S. Pittera, L. Raffaele, M. G. Sabini, V. Salamone, and L. M. Valastro, "Preliminary investigation on the use of the MOSFET dosimeter in proton beams," *Phys. Med.*, vol. 22, no. 1, pp. 29-32, 2006, doi: https://doi.org/10.1016/S1120-1797(06)80008-6.
[55] R. Kohno, K. Hotta, T. Matsuura, K. Matsubara, S. Nishioka, T. Nishio, M. Kawashima, and T. Ogino, "Proton dose distribution measurements using a MOSFET detector with a simple dose-weighted correction method for let effects," *J. Appl. Clin. Med. Phys.*, vol. 12, no. 2, 2011, doi: https://doi.org/10.1120/jacmp.v12i2.3431.
[56] S. Ruiz-Arrebola, R. Fabregat-Borrás, E. Rodríguez, M. Fernández-Montes, M. Pérez-Macho, M. Ferri, A. García, J. Cardenal, M. T. Pacheco, and J. Anchuelo, "Characterization of microMOSFET detectors for in vivo dosimetry in high-dose-rate brachytherapy with ^{192}Ir," *Medical Physics*, vol. 47, no. 5, pp. 2242-2253, 2020, doi: https://doi.org/10.1002/mp.14080.
[57] A. Sadeghi, B. Prestidge, J. M. Lee, I. Jurkovic, M. Simms, W. Bice, E. Walker, "Clinical use of a linear array MOSFET for urethral dose verification in prostate high dose rate brachytherapy," *ABS 27th annual Meeting*, poster paper, 2006.
[58] VT02 Datasheet (Rev. 2.2), Varadis, 2022.
[59] Z.-Y. Qi, X.-W. Deng, S.-M. Huang, L. Zhang, Z.-C. He, X. A. Li, I. Kwan, M. Lerch, D. Cutajar, P. Metcalfe, and A. Rosenfeld, "In vivo verification of superficial dose for head and neck treatments using intensity-modulated techniques," *Medical Physics*, vol. 36, no. 1, pp. 59-70, 2008, doi: https://doi.org/10.1118/1.3030951.
[60] J. Cayley, E. Engels, T. Charles, P. Bennetto, M. Cameron, J. Poder, D. Hausermann, J. Paino, D. Butler, D. Cutajar, M. Petasecca, A. Rosenfeld, Y.-R. E. Tan, and M. Lerch, "Establishing linearity of the MOSkin detector for ultra-high dose-per-pulse, very-high-energy electron radiotherapy using dose-rate-corrected EBT-XD film," *Applied Sciences*, vol. 15, no. 14, p. 8101, 2025, doi: https://doi.org/10.3390/app15148101.
[61] P. H. Halvorsen, "Dosimetric evaluation of a new design MOSFET in vivo dosimeter," *Medical Physics*, vol. 32, no. 1, pp. 110-117, 2005, doi: https://doi.org/10.1118/1.1827771.
[62] R. A. Kinhikar, P. K. Sharma, C. M. Tambe, U. M. Mahantshetty, R. Sarin, D. D. Deshpande, and S. K. Shrivastava, "Clinical application of a OneDose^{TM} MOSFET for skin dose measurements during internal mammary chain irradiation with high dose rate brachytherapy in carcinoma of the breast," *Physics in Medicine and Biology*, vol. 51, N263-N268, 2006, doi: https://doi.org/10.1088/0031-9155/51/14/N01.
[63] G. X. Ding, and C. W. Coffey, "Dosimetric evaluation of the OneDose^{TM} MOSFET for measuring kilovoltage imaging dose from image-guided radiotherapy procedures," *Medical Physics*, vol. 37, no. 9, pp. 4880-4885, 2010, doi: https://doi.org/10.1118/1.3483099.
[64] T. Cheung, M. J. Butson, and P. K. N. Yu, "Effects of temperature variation on MOSFET dosimetry," *Physics in Medicine and Biology*, vol. 49, N191-N196, 2004, doi: https://doi.org/10.1088/0031-9155/49/13/N02.
[65] S. H. Carbonetto, M. A. García Inza, J. Lipovetzky, E. G. Redin, L. Sambuco Salomone, and A. Faigón, "Zero temperature coefficient bias in MOS devices. Dependence on interface traps density, application to MOS dosimetry," *IEEE Transactions on Nuclear Science*, vol. 58, no. 6, pp. 3348-3353, 2011, doi: https://doi.org/10.1109/TNS.2011.2170430.
[66] M. Soubra, J. Cygler, and G. MacKay, "Evaluation of a dual bias metal oxide-silicon semiconductor field effect transistor detector as radiation dosimeter," *Medical Physics*, vol. 21, no. 4, pp. 567-572, 1994, doi: https://doi.org/10.1118/1.597314.
[67] S. Carbonetto, M. Garcia-Inza, J. Lipovetzky, M. Carra, E. Redin, L. Sambuco Salomone, and A. Faigon, "CMOS differential and amplified dosimeter with field oxide n-channel MOSFETs," *IEEE Transactions on Nuclear Science*, vol. 61, no. 6, pp. 3466-3471, 2014, doi: https://doi.org/10.1109/TNS.2014.2368361.
[68] M. Garcia-Inza, S. H. Carbonetto, J. Lipovetzky, and A. Faigon, "Radiation sensor based on MOSFETs mismatch amplification for radiotherapy applications," *IEEE Transactions on Nuclear Science*, vol. 63, no. 3, pp. 1784-1789, 2016, doi: https://doi.org/10.1109/TNS.2016.2560172.
[69] S. Carbonetto, M. Echarri, J. Lipovetzky, M. Garcia-Inza, and A. Faigón, "Temperature-compensated MOS dosimeter fully integrated in a high-voltage 0.35 μm CMOS process," *IEEE Transactions on Nuclear Science*, vol. 67, no. 6, pp. 1118-1124, 2020, doi: https://doi.org/10.1109/TNS.2020.2966567.
[70] H. E. Boesch, Jr., F. B. McLean, J. M. Benedetto, J. M. McGarrity, and W. E. Bailey, "Saturation of threshold voltage shift in MOSFET's at high total dose," *IEEE Transactions on Nuclear Science*, vol. 33, no. 6, pp. 1191-1197, 1986, doi: https://doi.org/10.1109/TNS.1986.4334577.
[71] E. H. Snow, A. S. Grove, and D. J. Fitzgerald, "Effects of ionizing radiation on oxidized silicon surfaces and planar devices," *Proceedings of the IEEE*, vol. 55, no. 7, pp. 1168-1185, 1967, doi: https://doi.org/10.1109/PROC.1967.5776.
[72] A. Kelleher, N. McDonnell, B. O'Neill, and W. Lane, "Investigation into re-use of PMOS dosimeters," *IEEE Transactions on Nuclear Science*, vol. 41, no. 3, pp. 445-451, 1994, doi: https://doi.org/10.1109/23.299782.
[73] A. Kelleher, W. Lane, and L. Adams, "Investigation of on-chip high temperature annealing of PMOS dosimeters," *IEEE Transactions on Nuclear Science*, vol. 43, no. 3, pp. 997-1001, 1996, doi: https://doi.org/10.1109/RADECS.1995.509821.
[74] G. Ristic, "Thermal and UV annealing of irradiated pMOS dosimetric transistors," *Journal of Physics D: Applied Physics*, vol.

42, 135001, 2009, doi: https://doi.org/10.1088/0022-3727/42/13/135101.

[75] E. Yilmaz, and R. Turan, "Temperature cycling of MOS-based radiation sensors," *Sensors and Actuators*, vol. 141, pp. 1-5, 2008, doi: https://doi.org/10.1016/j.sna.2007.07.001.

[76] L. Sambuco Salomone, M. V. Cassani, M. Garcia-Inza, A. Faigón, S. Carbonetto, and E. Redin, "Preliminary results of the thermal annealing for MOS dosimeters reutilization," *2025 Argentine Conference on Electronics (CAE), IEEE*, pp. 82-86, 2025, doi: https://doi.org/10.1109/CAE64243.2025.10961957.

[77] D. Verellen, S. Van Vaerenbergh, K. Tournel, K. Heuninckx, L. Joris, M. Duchareau, N. Linthout, T. Gevaert, T. Reynders, I. Van de Vondel, L. Coppens, T. Depuydt, M. De Ridder, and G. Storme, "An in-house developed resettable MOSFET dosimeter for radiotherapy," *Physics and Biology*, vol. 55, pp. 97-109, 2010, doi: https://doi.org/10.1088/0031-9155/55/4/N01.

[78] G.-W. Luo, Z.-Y. Qi, X.-W. Deng, and A. Rosenfeld, "Investigation of a pulsed current annealing method in reusing MOSFET dosimeters for in vivo IMRT dosimetry," *Medical Physics*, vol. 41, no. 5, 051710, 2014, doi: https://doi.org/10.1118/1.4871619.

[79] Y. Nissan-Cohen, J. Shappir, and D. Frohman-Bentchkowsky, "Dynamic model of trapping-detrapping in SiO_2," *Journal of Applied Physics*, vol. 58, no. 6, pp. 2252-2261, 1985, doi: https://doi.org/10.1063/1.335942.

[80] D. J. DiMaria, E. Cartier, and D. Arnold, "Impact ionization, trap creation, degradation, and breakdown in silicon dioxide films on silicon," *Journal of Applied Physics*, vol. 73, no. 7, pp. 3367-3384, 1993, doi: https://doi.org/10.1063/1.352936.

[81] D. Arnold, E. Cartier, and D. J. DiMaria, "Theory of high-field electron transport and impact ionization in silicon dioxide," *Physical Review B*, vol. 49, no. 15, pp. 10278-10297, 1994, doi: https://doi.org/10.1103/PhysRevB.49.10278.

[82] E. Miranda, E. Redin, and A. Faigon, "An effective field approach for the Fowler-Nordheim tunneling current through a metal-oxide-semiconductor charged barrier," *Journal of Applied Physics*, vol. 82, no. 3, pp. 1262-1265, 1997, doi: https://doi.org/10.1063/1.366535.

[83] J. Lipovetzky, E. G. Redin, and A. Faigon, "Electrically erasable metal-oxide-semiconductor dosimeters," *IEEE Transactions on Nuclear Science*, vol. 54, no. 4, pp. 1244-1250, 2007, doi: https://doi.org/10.1109/TNS.2007.895122.

[84] J. Lipovetzky, A. Holmes-Siedle, M. García Inza, S. Carbonetto, E. Redin, and A. Faigon, "New Fowler-Nordheim injection, charge neutralization, and gamma tests on the REM RFT300 RADFET dosimeter," *IEEE Transactions on Nuclear Science*, vol. 59, no. 6, pp. 3133-3140, 2012, doi: https://doi.org/10.1109/TNS.2012.2222667.

[85] D. M. Fleetwood, "Radiation induced charge neutralization and interface trap buildup in metal oxide semiconductor devices," *Journal of Applied Physics*, vol. 67, no. 1, pp. 580-583, 1990, doi: https://doi.org/10.1063/1.345199.

[86] A. Faigon, J. Lipovetzky, E. Redin, and G. Krusczenski, "Extension of the measurement range of MOS dosimeters using radiation induced charge neutralization," *IEEE Transactions on Nuclear Science*, vol. 55, no. 4, pp. 2141-2147, 2008, doi: https://doi.org/10.1109/TNS.2008.2000767.

[87] J. Lipovetzky, E. G. Redin, M. A. García Inza, S. Carbonetto, and A. Faigón, "Reducing measurement uncertainties using bias cycled measurement in MOS dosimetry at different temperatures," *IEEE Transactions on Nuclear Science*, vol. 57, no. 2, pp. 848-853, 2010, doi: https://doi.org/10.1109/TNS.2010.2042178.

[88] P. J. McWhorter, S. L. Miller, and W. M. Miller, "Modeling the anneal of radiation-induced trapped holes in a varying thermal environment," *IEEE Transactions on Nuclear Science*, vol. 37, no. 6, pp. 1682-1689, 1990, doi: https://doi.org/10.1109/23.101177.

[89] G. F. Derbenwick, and B. L. Gregory, "Process optimization of radiation-hardened CMOS integrated circuits," *IEEE Transactions on Nuclear Science*, vol. 22, no. 6, pp. 2151-2156, 1975, doi: https://doi.org/10.1109/TNS.1975.4328096.

[90] C. R. Viswanathan, and J. Maserjian, "Model for thickness dependence of radiation charging in MOS structures," *IEEE Transactions on Nuclear Science*, vol. 23, no. 6, pp. 1540-1545, 1976, doi: https://doi.org/10.1109/TNS.1976.4328535.

[91] N. S. Saks, M. G. Ancona, and J. A. Modolo, "Radiation effects in MOS capacitors with very thin oxides at 80 K," *IEEE Transactions on Nuclear Science*, vol. 31, no. 6, pp. 1249-1255, 1984, doi: https://doi.org/10.1109/TNS.1984.4333491.

[92] J. Lipovetzky, M. Garcia-Inza, S. Carbonetto, M. J. Carra, E. G. Redin, L. Sambuco Salomone, and A. Faigon, "Field oxide n-channel MOS dosimeters fabricated in CMOS processes," *IEEE Transactions on Nuclear Science*, vol. 60, no. 6, pp. 4683-4691, 2013, doi: https://doi.org/10.1109/TNS.2013.2287256.

[93] T. R. Oldham, A. J. Lelis, H. E. Boesch, J. M. Benedetto, F. B. McLean, and J. M. McGarrity, "Post-irradiation effects in field-oxide isolation structures," *IEEE Transactions on Nuclear Science*, vol. 34, no. 6, pp. 1184-1189, 1987, doi: https://doi.org/10.1109/TNS.1987.4337450.

[94] J. M. Terrell, T. R. Oldham, A, J. Lelis, and J. M. Benedetto, "Time dependent annealing of radiation-induced leakage currents in MOS devices," *IEEE Transactions on Nuclear Science*, vol. 36, no. 6, pp. 2205-2211, 1989, doi: https://doi.org/10.1109/23.45426.

[95] I. Sanchez Esqueda, H. J. Barnaby, K. E. Holbert, and Y. Boulghassoul, "Modeling inter-device leakage in 90 nm bulk CMOS devices," *IEEE Transactions on Nuclear Science*, vol. 58, no. 3, pp. 793-799, 2011, doi: https://doi.org/10.1109/TNS.2010.2101616.

[96] M. Garcia-Inza, M. Cassani, S. Carbonetto, M. Casal, E. Redin, and A. Faigon, "6 MV LINAC characterization of a MOSFET dosimeter fabricated in a CMOS process," *Radiation Measurements*, vol. 117, pp. 63-69, 2018, doi: https://doi.org/10.1016/j.radmeas.2018.07.009.

[97] J. Kassabov, N. Nedev, and N. Smirnov, "Radiation dosimeter based on floating gate MOS transistor," *Radiation Effects and Defects in Solids*, vol. 116, no. 1-2, pp. 155-158, 1991, doi: https://doi.org/10.1080/10420159108221354.

[98] C. J. Peters, N. G. Tarr, K. Shortt, I. Thomson, and G. F. MacKay, "A floating-gate MOSFET gamma dosimeter," *Canadian Journal of Physics*, vol. 74, no. 12, pp. 135-138, 1996, doi: https://doi.org/10.1139/p96-846.

[99] N. G. Tarr, G. F. MacKay, K. Shortt, and I. Thomson, "A floating gate MOSFET dosimeter requiring no external bias supply," *IEEE Transactions on Nuclear Science*, vol. 45, no. 3, pp. 1470-1474, 1998, doi: https://doi.org/10.1109/RADECS.1997.698909.

[100] N. G. Tarr, K. Shortt, Y. Wang, and I. Thomson, "A sensitive, temperature-compensated, zero-bias floating gate MOSFET dosimeter," *IEEE Transactions on Nuclear Science*, vol. 51, no. 3, pp. 1277-1282, 2004, doi: https://doi.org/10.1109/TNS.2004.829372.

[101] M. Martin, D. Roth, A. Garrison-Darrin, P. McNulty, and A. Andreou, "FGMOS dosimetry: Design and implementation," *IEEE Transactions on Nuclear Science*, vol. 48, no. 6, pp. 2050-2055, 2001, doi: https://doi.org/10.1109/23.983171.

[102] M. García Inza, J. Lipovetzky, E. G. Redin, S. Carbonetto, and A. Faigón, "Floating gate pMOS dosimeters under bias controlled cycled measurement," *IEEE Transactions on Nuclear Science*, vol. 58, no. 3, pp. 808-812, 2011, doi: https://doi.org/10.1109/TNS.2010.2099668.

[103] E. Garcia-Moreno, E. Isern, M. Roca, R. Picos, J. Font, J. Cesari, and A. Pineda, "Floating gate CMOS dosimeter with frequency output," *IEEE Transactions on Nuclear Science*, vol. 59, no. 2, pp. 373-378, 2012, doi: https://doi.org/10.1109/TNS.2012.2184301.

[104] E. Garcia-Moreno, E. Isern, M. Roca, R. Picos, J. Font, J. Cesari, and A. Pineda, "Temperature compensated floating gate MOS radiation sensor with current output," *IEEE Transactions on Nuclear Science*, vol. 60, no. 5, pp. 4026-4030, 2013, doi: https://doi.org/10.1109/TNS.2013.2277605.

[105] E. G. Villani, A. Gabrielli, A. Khan, E. Pikhay, Y. Roizin, and Z. Zhang, "Monolithic 180 nm CMOS dosimeter for in vivo medical applications," *IEEE Transactions on Nuclear Science*, vol. 60, no. 2, pp. 843-849, 2013, doi: https://doi.org/10.1109/TNS.2013.2251472.

[106] E. G. Villani, M. Crepaldi, D. DeMarchi, A. Gabrielli, A. Khan, E. Pikhay, Y. Roizin, A. Rosenfeld, and Z. Zhang, "A monolithic 180 nm CMOS dosimeter for wireless in vivo dosimetry," *Radiation Measurements*, vol. 84, pp. 55-64, 2016, doi: https://doi.org/10.1016/j.radmeas.2015.11.004.

[107] M. Brucoli, S. Danzeca, M. Brugger, A. Masi, A. Pineda, J. Cesari, L. Dusseau, and F. Wrobel, "Floating gate dosimeter suitability for accelerator-like environments," *IEEE Transactions on Nuclear Science*, vol. 64, no. 8, pp. 2054-2060, 2017, doi: https://doi.org/10.1109/TNS.2017.2681651.

[108] C. Zhang, and S. M. Rezaul Hasan, "A new floating-gate radiation sensor and readout circuit in standard single-poly 130-nm CMOS technology," *IEEE Transactions on Nuclear Science*, vol. 66, no. 7, pp. 1906-1915, 2019, doi: https://doi.org/10.1109/TNS.2019.2922714.

[109] T. Darós, N. C. Cábia, J. Piteira, and M. C. Schneider, "Design, modeling, and characterization of a floating gate dosimeter in standard CMOS technology for sensor reuse," *IEEE Transactions on Nuclear Science*, vol. 72, no. 2, pp. 3069-3076, 2025, doi: https://doi.org/10.1109/TNS.2025.3594306.

[110] L. Z. Scheick, P. J. McNulty, and D. R. Roth, "Dosimetry based on the erasure of floating gates in the natural radiation environments in space," *IEEE Transactions on Nuclear Science*, vol. 45, no. 6, pp. 2681-2688, 1998, doi: https://doi.org/10.1109/23.736515.

[111] P. J. McNulty, M. Rajaman, K. F. Poole, K. R. Freeman, J. P. Dyar, L. Z. Scheick, M. Alkhafazi, and M. G. Randall, "Simplified readout of UVPROM dosimeters for spacecraft applications," *IEEE Transactions on Nuclear Science*, vol. 53, no. 4, pp. 1859-1862, 2006, doi: https://doi.org/10.1109/TNS.2006.877564.

[112] P. J. McNulty, and K. F. Poole, "Increasing the sensitivity of FGMOS dosimeters by reading at higher temperature," *IEEE Transactions on Nuclear Science*, vol. 59, no. 4, pp. 1113-1116, 2012, doi: https://doi.org/10.1109/TNS.2012.2192288.

[113] R. Edgecock, J. Matheson, M. Weber, E. G. Villani, R. Bose, A: Khan, D. R. Smith, I. Adil-Smith, and A. Gabrielli, "Evaluation of commercial programmable floating gate devices as radiation dosimeters," *Journal of Instrumentation*, vol. 4, no. 2, pp. 1-10, 2009, doi: https://doi.org/10.1088/1748-0221/4/02/P02002.

[114] S. Ilić, A. Jevtić, S. Stanković, and G. Ristić, "Floating-gate MOS transistor with dynamic biasing as a radiation sensor," *Sensors*, vol. 20, no. 11, p. 3329, 2021, doi: https://doi.org/10.3390/s20113329.

[115] S. Ilić, M. S. Andjelković, R. Duane, A. J. Palma, M. Sarajlić, S. Stanković, and G. R. Ristić, "Recharging process of commercial floating-gate MOS transistor in dosimetry application," *Microelectronics Reliability*, vol. 126, p. 114322, 2022, doi: https://doi.org/10.1016/j.microrel.2021.114322 .